High-Order Lowpass Filters Using DVCC Elements

Josef ČAJKA[1], Tomáš DOSTÁL[2], Kamil VRBA[1]

[1] Dept. of Telecommunications
[2] Dept. of Radio Electronics
Brno University of Technology
Purkyňova 118, 612 00 Brno
Czech Republic

Abstract

Special cells using a differential voltage current conveyor are presented. The use of these cells for high-order lowpass filter design is described. The filters can be designed to operate in different modes.

Keywords

Analogue circuits, current conveyors, lowpass filters, antialiasing filters.

1. Introduction

The high-order lowpass filters are frequently used as antialiasing filters [1]. The transfer function of an *n*th-order lowpass filter is defined as follows

$$H(s) = b_0 \Big/ \sum_{i=0}^{n} a_i s^i \quad . \tag{1}$$

Here s is the complex frequency variable, b_i and a_i are polynomial coefficients.

We have proposed a simple algorithm for *n*th-order lowpass filter design with a minimum number of active and passive elements and with the canonical form of the transfer function. The proposed network is based on the five-port zero-class current conveyor (usually denoted as DVCC - differential voltage current conveyor [2]), which is defined by the following equation set:

$$V_x = V_{y+} - V_{y-} \quad ,$$

$$I_x = I^* \quad ,$$

$$I_{y+} = I_{y-} = 0 \quad \text{(zero-class condition)},$$

$$I_{z+} = +I^* \quad ,$$

$$I_{z-} = -I^* \quad ,$$

where I^* is independent current. Symbols x, $y+$, $y-$, $z+$, $z-$ denote the appropriate node terminals of the active DVCC device.

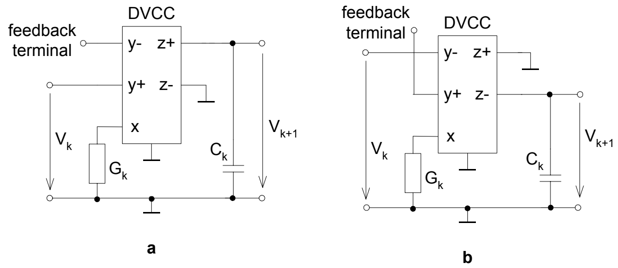

Fig. 1 Basic cells for voltage-mode filter design

2. Design procedure

Let us consider the simple building cell containing a DVCC element shown in Fig. 1a, b. The subscript k in the figure indicates the serial number of the cell in a cascade connection. When the feedback terminal of both cells is grounded, we get their simple voltage transfer function

$$V_{k+1}/V_k = G_k / (sC_k) \quad . \tag{2}$$

The *voltage* building cells in Fig. 1a,b can be easily transformed into their adjoint counterparts [3], i.e. into the *current* building cells drawn in Fig. 2a, b. Here we are considering currents instead of voltages, having interchanged the input-port with the output-port and having interchanged the following conveyor terminals: $y+ \Leftrightarrow z-$ and $y- \Leftrightarrow z+$. The symbol $\Leftrightarrow$ relates to the mutual port interchange. The current transfer function of both cells in Fig. 2a, b is also given by the right-hand side of eqn. (2).

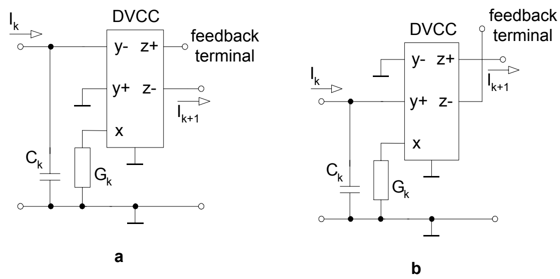

Fig. 2 Basic cells for current-mode filter design

If we connect n cells with grounded feedback terminals acc. to Fig 1 (cells in Fig. 1a can be arbitrarily combined with cells in Fig. 1b) in cascade, the voltage transfer function of the whole two-port network can be written in the following form

$$\frac{V_{out}}{V_{in}} = \frac{1}{s^n} \prod_{k=1}^{n} \frac{G_k}{C_k} \quad . \tag{3}$$

To expand the denominator of (3), we will use the feedback terminals of individual cells. *All* the feedback connections start from the *output terminal*. If the feedback

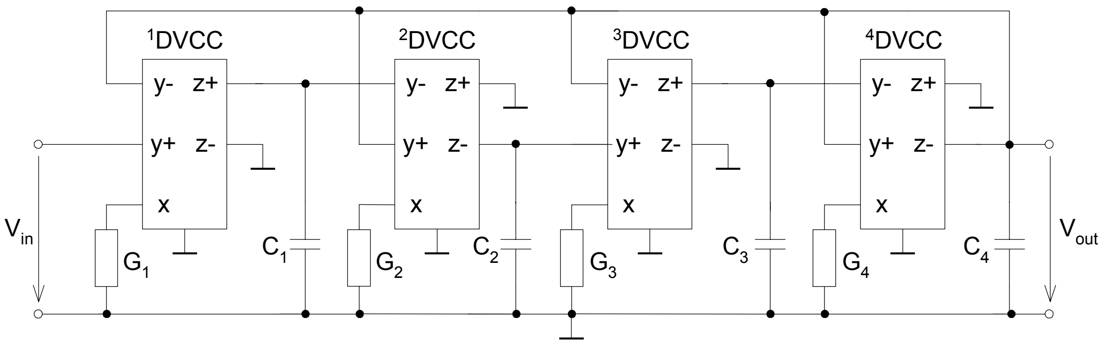

Fig. 3 A fourth-order lowpass filter operating in the voltage mode

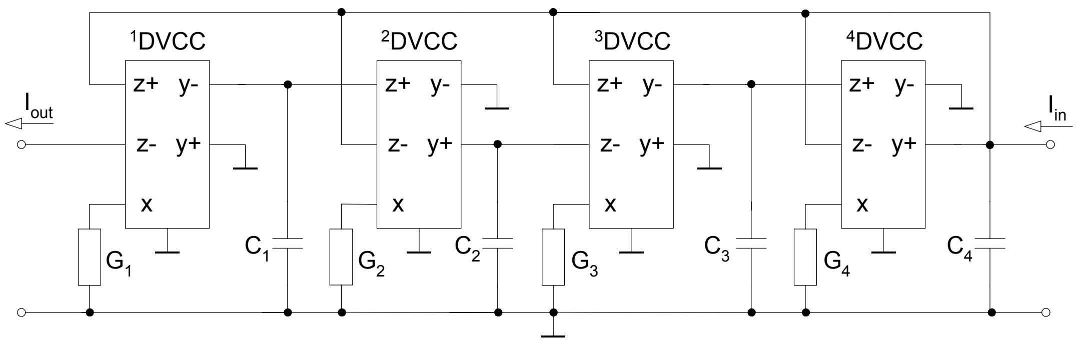

Fig. 4 The lowpass filter operating in the current mode derived from that in Fig. 3

is fed to the first cell of the cascade, the following additional term in denominator will be obtained:

$$\prod_{k=1}^{n} G_k \ , \tag{4}$$

whereas if the feedback is going to the second cell, we can write: $sC_1\,\Pi^{n}{}_{k=2}\,G_k$, and the feedback to the 3rd cell gives $s^2\,C_1C_2\,\Pi^{n}{}_{k=3}\,G_k$, and $(s^{n-1}\,\Pi^{n-1}{}_{k=1}\,C_k)\,G_k$. It means that all the feedback terminals of the cells in cascade must be connected with the live output terminal node. As an example, a fourth-order lowpass filter operating in the voltage mode is shown in Fig. 3.

The Fig. 4 presents the same filter operating in the current mode. We have transformed the network in Fig. 3 using adjoint voltage-to-current network transformation. We get the same structure if we connect 4 building cells in Fig. 2a or in Fig. 2b in cascade and if we simultaneously interconnect the iput terminal with all feedback terminals in the cascade. The polynomial coefficients, see eqn. (1), for both the above filters are:

$$b_0 = a_0 = G_1G_2G_3G_4 \ , \quad a_1 = C_1G_2G_3G_4 \ ,$$
$$a_2 = C_1C_2G_3G_4 \ , \qquad a_3 = C_1C_2C_3G_4 \ ,$$
$$a_4 = C_1C_2C_3C_4 \ .$$

If an lowpass filter operating in the transadmittance mode is required, we can load the output port of a voltage mode filter by a two-port network as shown in Fig. 5. The *transadmittance* function of this two-port is:

$$\frac{I_{out}}{V_{in}} = G_3\,\frac{G_1G_2}{G_1G_2 + sC_1G_2 + s^2C_1C_2} \tag{5}$$

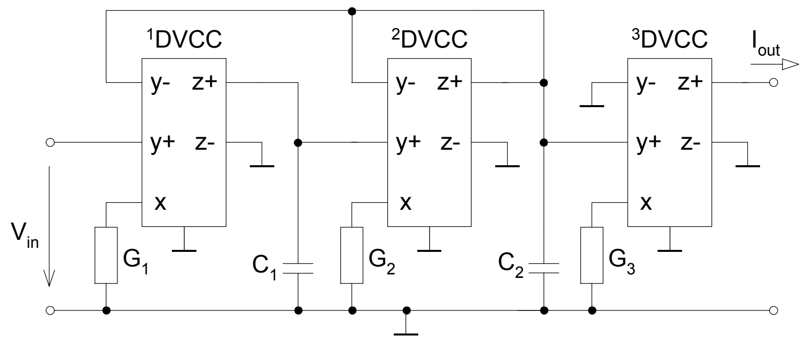

Fig. 5 A second-order lowpass filter operating in the transadmittance mode

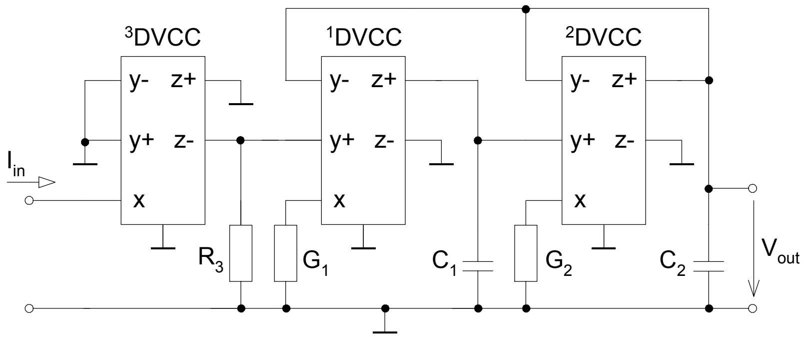

Fig. 6 A second-order lowpass filter operating in the transimpedance-mode

On the other hand, the network diagram in Fig. 6 shows the realization of a lowpass filter, which operates in the *transimpedance* mode. The transfer function of this filter is defined by the following equation:

$$\frac{V_{out}}{I_{in}} = R_3 \frac{G_1 G_2}{G_1 G_2 + sC_1 G_2 + s^2 C_1 C_2} \ . \qquad (6)$$

For the n^{th}-order voltage/current mode lowpass filter design we need only n DVCC devices, n grounded capacitors and n grounded resistors. We can formulate a simple rule for the transfer function formulation in canonical form: In the numerator we write the product of all cell conductances (4). If, e.g., $n = 6$, we get: $b_0 = G_1 G_2 G_3 G_4 G_5 G_6$.

The denominator has $n+1$ terms. The first one is the same as in the numerator. In the following terms we replace successively those conductances by corresponding capacitor admittances of cells through which the signal has been already passed. Using the above example we can write the following denominator coefficients:

$$\begin{aligned} a_0 &= G_1G_2G_3G_4G_5G_6, \quad a_1 = C_1G_2G_3G_4G_5G_6, \\ a_2 &= C_1C_2G_3G_4G_5G_6, \quad a_3 = C_1C_2C_3G_4G_5G_6, \\ a_4 &= C_1C_2C_3C_4G_5G_6, \quad a_5 = C_1C_2C_3C_4C_5G_6, \\ a_6 &= C_1C_2C_3C_4C_5C_6. \end{aligned} \qquad (7)$$

Let's note that all the passive filter elements are grounded.

If we need a filter operating in the combined mode, we must add a transforming two-port consisting of one DVCC element and one resistor.

3. Filter realisation and simulation

To illustrate the given design procedure, an audio filter with this specification was chosen:

- 6^{th}-order, lowpass,
- Butterworth approximation (maximally flat),
- cut-off frequency f_c = 16 kHz at –3 dB,
- stop-band frequency f_s = 75 kHz at –80 dB.

In the first step following coefficients of the desired transfer function (1) were obtained using NAF computer tool:

$$\begin{aligned} b_0 = a_0 &= 1.002377 \\ a_1 &= 3.871356 \cdot 10^{-5} \\ a_2 &= 7.475927 \cdot 10^{-10} \\ a_3 &= 9.1524806 \cdot 10^{-15} \\ a_4 &= 7.470012 \cdot 10^{-20} \\ a_5 &= 3.865233 \cdot 10^{-25} \\ a_6 &= 10^{-30}. \end{aligned} \qquad (8)$$

Then substituting the coefficients from (8) into (7) and choosing some values of the capacitances, the resulting circuit of the structure given in Fig. 3, but with six cells of the DVCC, has the following values of the components:

$$\begin{aligned} &C_1 = C_2 = C_3 = C_4 = C_5 = C_6 = 1 \text{ nF}, \\ &R_1 = 38.62 \text{ k}\Omega,\ R_2 = 19.31 \text{ k}\Omega,\ R_3 = 12.24 \text{ k}\Omega, \\ &R_4 = 8.16 \text{ k}\Omega,\ R_5 = 5.17 \text{ k}\Omega,\ R_6 = 2.58 \text{ k}\Omega. \end{aligned} \qquad (9)$$

This filter was simulated by means of the PSpice, using a suitable model of the ideal DVCC, namely with controlled CCCS and VCVS sources only [4]. The resulting magnitude response is shown in Fig. 7. This simulation confirms symbolical analysis and theoretical assumptions.

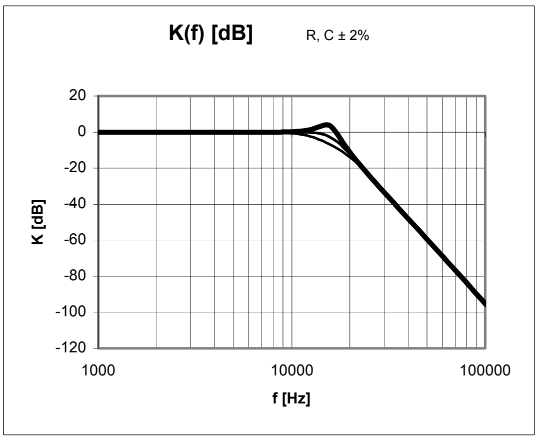

Fig. 7 Magnitude responses of the 6^{th}-order, audio, DVCC-based filter, nominal and worst case tolerance analysis for the tolerances of the Rj and Cj δ = ± 2%

In Fig. 7, the result of the statistical analysis is shown too, namely for the tolerances of all passive components R_j

and C_j $\delta = \pm 2$ %. Comparing this with the standard opamp-based filter, we must admit that its sensitivity is higher, which is typical of this type of structure and which is given by the construction of the transfer coefficients in (7). Note that the tolerances of passive elements larger than ± 5 % cannot be used, due to a very great distortion of the magnitude response.

Furthermore, to evaluate the performance of above structure in the HF range, another video filter was taken, with the following specification:

- 6^{th}-order, lowpass,
- Bessel approximation, linear phase (flat delay),
- cut-off frequency f_c = 5 MHz at –3 dB,
- stop-band frequency f_s = 15 MHz at –30 dB

The design equations (7) are now:

$$b_0 = a_0 = 1$$
$$a_1 = 8.5914 \cdot 10^{-8} = C_1 R_1$$
$$a_2 = 3.3551 \cdot 10^{-15} = C_1 C_2 R_1 R_2$$
$$a_3 = 7.6872 \cdot 10^{-23} = C_1 C_2 C_3 R_1 R_2 R_3 \qquad (10)$$
$$a_4 = 1.1007 \cdot 10^{-30} = C_1 C_2 C_3 C_4 R_1 R_2 R_3 R_4$$
$$a_5 = 9.4562 \cdot 10^{-39} = C_1 C_2 C_3 C_4 C_5 R_1 R_2 R_3 R_4 R_5$$
$$a_6 = 3.8687 \cdot 10^{-47} = C_1 C_2 C_3 C_4 C_5 C_6 R_1 R_2 R_3 R_4 R_5 R_6$$

Then the resulting values of the circuit components are:

$$C_1 = C_2 = C_3 = C_4 = C_5 = C_6 = 100 \text{ pF},$$
$$R_1 = 859.1\ \Omega,\ R_2 = 390.5\ \Omega,\ R_3 = 229.1\ \Omega,$$
$$R_4 = 143.1\ \Omega,\ R_5 = 85.9\ \Omega,\ R_6 = 40.9\ \Omega. \qquad (11)$$

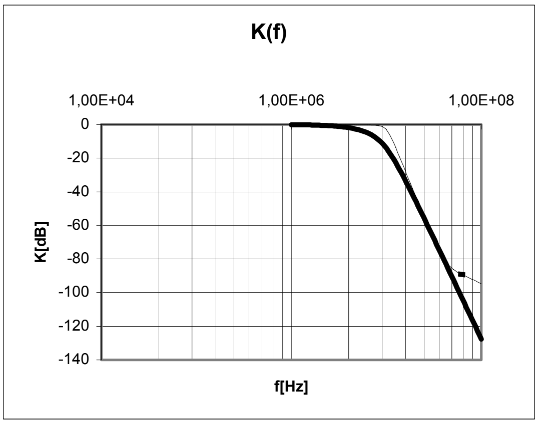

Fig. 8 Magnitude frequency responses of the 6^{th}-order video DVCC-based filter, with the ideal and real DVCC.

This filter was simulated by means of the PSpice too, using the 3-rd level frequency-dependent ABM model [4] of the real DVCC. The resulting magnitude frequency responses are shown in Fig. 8, namely one - thick curve, for the ideal DVCC and the other one - thin curve, for the real DVCC, with the parasitic input resistance of the current port R_x = 5 Ω, the cut-off (-3 dB) frequency f_{mV} = 60 MHz of the voltage buffering and similarly f_{mC} = 80 MHz for the current buffering.

According to our experience, the parasitic input resistance R_x of the real DVCC plays a most important role. It is illustrated in Fig. 9, which gives the resulting parametric AC analysis of this video filter. It shows how *K(f)* changes with resistor R_x, from zero to 50 Ω, in steps of 10 Ω respectively.

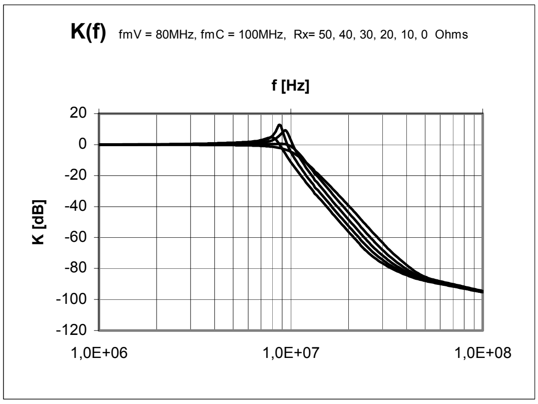

Fig. 9 Magnitude responses of the 6^{th} –order video filter using the real DVCC with f_{mV} = 80MHz, f_{mC} = 100MHz and R_x varying from zero to 50 Ohms.

4. Conclusion

Basic cells using five-port current conveyors and the direct design of high-order LP filters were presented. On one hand the proposed algorithm is simple and designed filter has a minimum number of active and passive elements, but we must accept a higher sensitivity than standard ARC filters have. It was shown by PSpice simulations that the filters constructed by proposed method gave frequency responses near the theoretical one. They are really the right choice for the HF range, with a lower influence of parasitic parameters, especially in the current mode.

Acknowledgements

This work was supported by the Grant Agency of the Czech Republic (GAČR) (grants No. 102/00/2037, No. 102/01/0228) and by the Ministry of Education of the Czech Republic (program CEZ-J22/98:262200011).

References

[1] VRBA, K., ČAJKA, J. Antialiasing filters using new active elements. In Proceedings of the Euroconference Biosignal 2000. Brno, 2000, p.180 - 182

[2] ELWAN, H. O., SOLIMAN, A. M. Novel CMOS differential voltage current conveyor and its application. IEE Proceedings - Circuits Devices Syst. 1997, vol. 144, no. 3, p. 195 - 200.

[3] DOSTÁL, T., VRBA, K., ČAJKA, J. Adjoint voltage-to-current network transformation. In Proc. of the Conference RADIOELEKTRONIKA 2000. Bratislava, 2000, p. I8 - I10.

[4] DOSTÁL, T. Modeling of modern active devices for simulation of analog circuits in PSpice. Radioengineering. 2000, vol. 9, no. 3, p. 8 - 11.